EMERGING METHODS AND TECHNOLOGIES

Analytical methods for the investigation of enzyme-catalyzed degradation of polyethylene terephthalate

Valentina Pirillo, Loredano Pollegioni [ID] and Gianluca Molla

The Protein Factory 2.0', Dipartimento di Biotecnologie e Scienze della Vita, Università degli Studi dell'Insubria, Varese, Italy

The polyester PET (poly(ethylene terephthalate)) plastic is chemically inert and remarkably persistent, posing relevant and global pollution concerns due to its accumulation in ecosystems across the globe. In past years, research focused on identifying bacteria active on PET and on the specific enzymes responsible for its degradation. Here, the enzymatic degradation of PET can be considered as an 'erosion process' that takes place on the surface of an insoluble material and results in an unusual, substrate-limited kinetic condition. In this review, we report on the most suitable models to evaluate the kinetics of PET-hydrolyzing enzymes, which takes into consideration the amount of enzyme adsorbed on the substrate, the enzyme-accessible ester bonds, and the product inhibition effects. Careful kinetic analysis is especially relevant to compare enzymes from different sources and evolved variants generated by protein engineering studies as well. Furthermore, the analytical methods most suitable to screen natural bacteria and recombinant variant libraries generated by protein engineering have been also reported. These methods rely on different detection systems and are performed both on model compounds and on different PET samples (e.g., nanoparticles, microparticles, and waste products). All this meaningful information represents an optimal starting point and boosts the process of identifying systems able to biologically recycle PET waste products.

Introduction

During the 20th century, plastics became central to human life, based on their unbelievable versatility and low cost. However, the massive production and use of plastics together with their very long persistence pose an extreme global pollution threat, especially in marine environments [1–5]. Poly(ethylene terephthalate) (PET), the most plentiful man-made polyester plastic in the world (with a predicted life time of 25–50 years) [6], is used to produce textile fibers and resins for single-use beverage bottles and packaging. This thermoplastic polymer is composed of terephthalic acid (TPA) and ethylene glycol (EG). Although PET can be depolymerized into its constituents via chemical processes based on the cleavage of the ester bonds under harsh conditions, such as the use of sulfuric acid at 150 °C [7,8] or under alkaline conditions in the presence of hazardous chemical catalysts (e.g., methyltrioctylammonium bromide) [9], at present PET is

primarily mechanically recycled, a process resulting in a loss of material properties and value. In this regard, and based on their great ability to adapt, some microorganisms are able to degrade plastics by evolving enzymes and catabolic pathways [10–13].

In 2016, a newly discovered bacterium, *Ideonella sakaiensis* 201-F6, was reported to use PET as a major carbon and energy source for growth [11], generating considerable media hype. The enzyme PETase (PET-digesting enzyme, EC 3.1.1.101) converts PET to mono(2-hydroxyethyl) terephthalic acid (MHET), with trace amounts of TPA and bis(2-hydroxyethyl)-TPA as secondary products, and the enzyme MHETase (MHET-digesting enzyme, EC 3.1.1.102) further converts MHET into the two monomers TPA and EG (Fig. 1). For the sake of completeness, we should mention that some previous studies also reported on microorganisms (such as the filamentous fungi *Fusarium oxysporum* and *F. solani*) [14,15] and enzymes [16–22] that can degrade PET.

A number of cutinases (EC 3.1.1.74), lipases (EC 3.1.1.3), and esterases (EC 3.1.1.x) are active on PET (for a review, see Ref. [23]): Cutinases have shown the greatest promise and thermostable biocatalysts are promising candidates. In recent years, evolved enzymes were generated by protein engineering studies. This is a powerful approach whose success is largely governed by a well-suited screening procedure (according to the dogma 'you get what you screen for').

PETase activity can be assayed using different methods. Some of these methods are based on the use of model compounds, such as oligomeric PET models (i.e., ethylene glycol dibenzyl ester, PET dimer and trimer), others are based on the use of functionalized esters [i.e., 4-nitrophenyl acetate (pNPA),

mono(2-hydroxyethyl)terephthalate, for which hydrolysis can be directly recorded; see Table 1], and yet others rely on the use of polymeric PET. For the sake of clarity, we need to mention that some model substrates, such as pNPA and 4-nitrophenyl butyrate (pNPB), are not realistic of the complex (hydrophobic and insoluble) structure of PET and their use should be considered for preliminary assays only (e.g., to check the amount of active enzyme during purification procedures or inactivation experiments). Additional methods useful for investigating PET degradation, but not suitable for screening, are represented by analysis of the polymer before and after the treatment by scanning electron microscopy imaging (to evaluate alterations in the polymeric structure) and by differential scanning calorimetry (to evaluate the degree of crystallinity). Recently, solution nuclear magnetic resonance (NMR) was employed to investigate the effect of the enzyme-catalyzed hydrolysis of PET on the chemical microstructure of the polymer. The NMR analysis allows the determination of the degree of polymerization of PET which, correlated with the amount of weight loss of the sample during the enzymatic treatment, allows the discrimination between the endo- and exo-type cleavage of the polymer [24]. In addition, the analysis of the PET properties at an atomic level (e.g., the determination of the ratio between the gauche and trans conformations in the polymer, which correlates with its degree of crystallinity) can be performed by solid-state NMR methods [25,26]. These methods give an in-depth assessment of the effect of enzymatic treatment on the polymer structure and are most suited for a detailed mechanistic investigation of the mode of action of PET hydrolases.
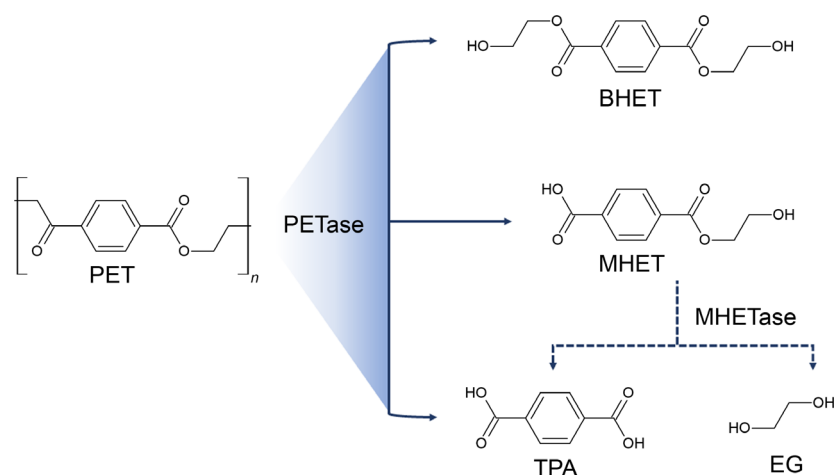

Fig. 1. Enzymatic hydrolysis of PET by PETases and MHETases. The ratio between the products can be different depending on the specific enzyme employed.

Table 1. Model substrates employed for the functional assays of PET hydrolytic enzymes.

Compound	Abbreviation	Physical form	Structure	MW (g·mol⁻¹)	Hydrolysis products	Detection of reaction products
4-Nitrophenyl acetate	pNPA	Powder(soluble in 100% EtOH)		181.15	4-Nitrophenol (pNP) + acetate	• Spectrophotometric detection (405 nm) • pH-based assay
4-Nitrophenyl butyrate[a]	pNPB	Powder (soluble in 100% EtOH)		209.20	4-Nitrophenol (pNP) + butyrate	• Spectrophotometric detection (405 nm) • pH-based assay
Mono(2-hydroxyethyl) terephthalate	MHET	Powder (soluble in DMSO)		209.17	TPA + EG	• UV absorption (240 nm) • HPLC
Bis(2-hydroxyethyl) terephthalate	BHET	Powder (soluble in DMSO)		254.24	(i) TPA + EG (ii) MHET + TPA + EG	• UV absorption (240 nm) • HPLC • pH-based assay
Ethylene glycol bis-(p-methylbenzoate)	2PET	Nanoparticles (suspension)		298.34 (Ø = ~ 320 nm)	4-Methylbenzoic acid	• Turbidimetric analysis
Poly(ethylene terephthalate)	PET	Nanoparticles (suspension)		Variable (Ø = 50–300 nm)	(i) TPA + EG (ii) MHET + TPA + EG	• UV absorption (240 nm) • Turbidimetric analysis
		Microparticles (insoluble)		Variable (Ø = 50–300 µm)	(i) TPA + EG (ii) MHET + TPA + EG	• UV absorption (240 nm) • pH-based assay • HPLC
		Granulate, films or fibers (insoluble)		Variable	(i) TPA + EG (ii) MHET + TPA + EG	• UV absorption (240 nm) • pH-based assay • HPLC

[a]Fatty acid ester chains up to 18 (pNP-stearate) carbons in length have been also used [43].

In this review, we present the state of the art of analytical methods useful for assaying PET hydrolytic enzymes, both novel and engineered variants. Furthermore, we emphasize that the ensuing kinetic data must be evaluated using a model for an insoluble substrate where the reaction is limited to the surface of the substrate (i.e., a 'substrate-limited' condition). These approaches and models cannot be translated to the investigation of the degradation process mediated by microorganisms, requiring longer times and frequently suffering from further degradation of the depolymerization products. Indeed, kinetic models for enzymatic reactions are limited to the initial phase of reaction and the effect of time is less appreciated.

Kinetic model of the heterogeneous enzymatic hydrolysis of PET

PET hydrolytic enzymes are classified into two major phylogenetic groups: type I and type II (which is further divided into the a and b subtypes) [27,28]. Although possessing different structural properties (type I and type II enzymes share ~ 50% of sequence identity), all PET hydrolases possess the same catalytic mechanism, typical of the α/β serine hydrolases with a charge–relay network (formed by an histidine and an aspartate) that activates the nucleophilic γ-OH of a serine side chain. The polymeric substrate is bound through several noncovalent interactions (mainly hydrophobic, π-π stacking interactions, and H-bonds) into a long cleft (~ 40 Å) on the surface of the enzyme, which can be divided into four subsites (I, IIa, IIb, and IIc) (Fig. 2) [27,28].

The enzymatic hydrolysis of insoluble PET particles (e.g., micro- or nanoparticles, films, and yarns) is a two-state heterogeneous reaction, and the corresponding reaction rate is limited by the enzyme-accessible surface area of the substrate (i.e., a substrate-limited condition) [29]. Under these conditions, the canonical Michaelis--Menten (M&M) kinetic model (that describes homogeneous reactions under enzyme-limited conditions) cannot be applied to determine the kinetic parameters. An alternative two-step kinetic model has been proposed that takes into account the partitioning of the enzyme between the soluble (free) and the substrate-adsorbed fractions [30–32]. This kinetic model can be applied for the analysis of kinetic data both for type I and for type II PET hydrolases. The kinetic model is formally analogous to that of M&M, in which binding is followed by hydrolysis and is based on eqn. 1:

$$E + S \underset{k_{-1}}{\overset{k_1}{\rightleftharpoons}} ES \xrightarrow{k_2} EP \underset{K_p}{\rightleftharpoons} E + P \tag{1}$$
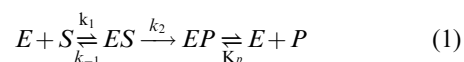
The equilibrium between the free and substrate-adsorbed enzyme fractions is defined by the absorption constant:
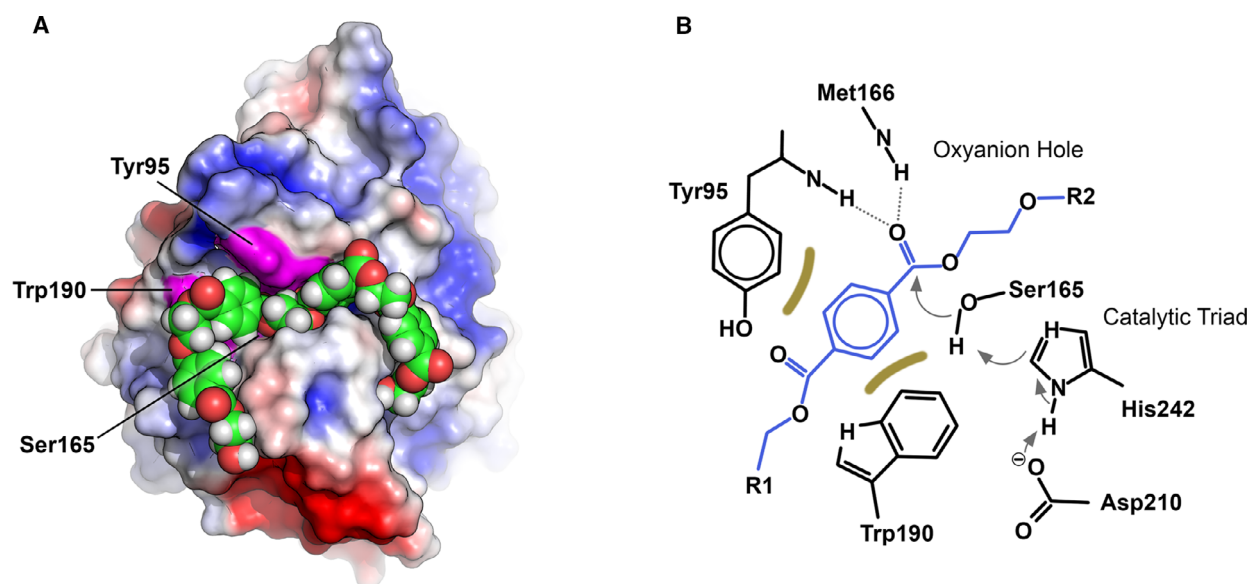
Fig. 2. Structural details of a PET-hydrolyzing enzyme. (A) Representation of a model of the complex between LCC (PDB code 4EB0) and a PET molecule. Negative and positive charged regions on the protein surface are colored in red and blue, respectively. Trp190 and Tyr95 are highlighted in purple, and the catalytic Ser165 is highlighted in cyan. (B) Details of the reaction mechanism of LCC [28]: Hydrophobic stacking interactions are shown by ocher thick lines, and PET is depicted in blue.

$$K_A (\mu M^{-1}) \text{ or } (\mu g/mL)^{-1} = \frac{[E_{adsorbed}]}{[E_{free}][PET_{binding sites}]} = k_1/k_{-1}$$

In addition, as only the superficial ester bonds are accessible to the enzyme, the initial reaction rate directly correlates with the surface of the insoluble substrate PET.

In analogy to the canonical M&M model, the initial reaction rate in the process proposed by Ref. [30] depends on the concentration of the ES complex and on its hydrolysis rate constant k_2 (expressed as $\mu mol \cdot cm^{-2} \cdot h^{-1}$ or $\mu g \cdot cm^{-2} \cdot h^{-1}$):

$$v_0 = k_2 [ES] \tag{2}$$

Since $[ES]$ is directly related to the substrate area that is bound to the enzyme, eqn. 2 can be rewritten as:

$$v_0 = k_2 A_0 \theta \tag{3}$$

where A_0 (expressed as μM or as reported by several authors as cm^2 or $cm^2 \cdot mL^{-1}$) is the concentration of the initial surface area of the polymer [31]. According to a Langmuir-type isotherm model for the adsorption of enzymes on insoluble substrates, the fraction of surface ester bonds that form a complex with the enzyme, named θ, depends on the enzyme concentration in solution ($[E]$) and on the adsorption equilibrium constant (K_A), according to the following equation [32]:

$$\theta = \frac{K_A[E]}{1 + K_A[E]} \tag{4}$$

Combining eqn. 3 with eqn. 4:

$$v_0 = k_2 A_0 \frac{K_A[E]}{1 + K_A[E]} \tag{5}$$

By interpolating the plot of v_0 as a function of the enzyme concentration using eqn. 5, the adsorption constant K_A and the hydrolysis rate constant k_2 can be determined (Fig. 3A). The adsorption constant K_A, which corresponds to K_S ($= k_1/k_{-1}$), is used as the 'canonical term' for the thermodynamic constant for a complex dissociation, and as such, it is a measure of the inverse of the affinity of the enzyme for the surface of the polymer.

Equation 5 describes a hyperbolic curve of the reaction rate (v_0) as a function of the enzyme concentration ($[E]$); therefore, at low $[E]$, v_0 increases linearly with the enzyme concentration, showing a first-order kinetic behavior, while at high $[E]$, v_0 reaches saturation (zero-order kinetic) (Fig. 3A, left). Equation 5 can also be used to interpolate values of v_0 measured at increasing substrate areas (A_0), provided that the $[E]$ is kept constant (Fig. 3A, right). The gap between the experimental and theoretical values observed at high PET concentration in the latter plot confirms that eqn. 5 can be applied only under substrate-limiting conditions [33].

The kinetic model of Ref. [30] was improved by adding the molar density of the ester bond (ρ_{EB}) parameter to eqn. 5. Accordingly, in a reaction mixture formed by a heterogeneous system (e.g., in the presence of a suspension of nanoPET particles), the initial reaction rate can be defined as the decrease in (enzyme-accessible) ester bonds η_{EB}:

$$v_0 = -\frac{d(\eta_{EB})}{dt} = k_2 \rho_{EB} A_0 \frac{K_A[E]}{1 + K_A[E]} \tag{6}$$

Equation 6 can be further improved by taking into account enzyme loading at the surface of the polymer substrate [34]. However, introducing this additional parameter renders application of the resulting equation more complex because it requires further information about the system under investigation. In addition, the improved model proposed by Ref. [34] is more suitable to describe rapid polyester hydrolysis, while Ronkvist and coauthors demonstrated that eqn. 5 is better suited to describe the relatively slow enzymatic degradation of PET [31].

By determining the kinetic parameters on PET using eqn. 6, researchers are provided with a quantitative tool to compare performances of PET hydrolysis between enzymes from different sources or between different variants of the same enzyme. For example, based on analysis of the reaction rate data collected by pH-Stat it was reported that the cutinase from *H. inso-lens* possessed the highest activity (i.e., the highest $k_2 = 0.62 \mu mol \cdot cm^{-2} \cdot h^{-1}$), while cutinase from *P. mendocina* showed the best affinity for PET (i.e., the highest $K_A = 0.76 \mu M^{-1}$) [31]. Silva *et al.* [35] increased the space and hydrophobicity of the binding cleft of *Thermobifida fusca* cutinase (Tfu_0883) introducing the two substitutions Q132A and T101A. Using an enzymatic fluorometric assay, the authors demonstrated that the substitutions enhanced the efficiency of PET hydrolysis by increasing both the adsorption equilibrium constant and the hydrolysis rate constant (5.3- and 9.0-fold, respectively; $K_A = 2.54 \mu M^{-1}$ and $k_2 = 6.63 \mu mol \cdot cm^{-2} \cdot h^{-1}$). The same authors showed that the surface-accessible ester bonds of PET are usually hydrolyzed within the first hours of reaction. After this time interval, the sites on the surface of PET where the enzyme can bind and hydrolyze the polymer ester bonds become fully occupied by the adsorbed enzyme itself, halting the reaction [35].
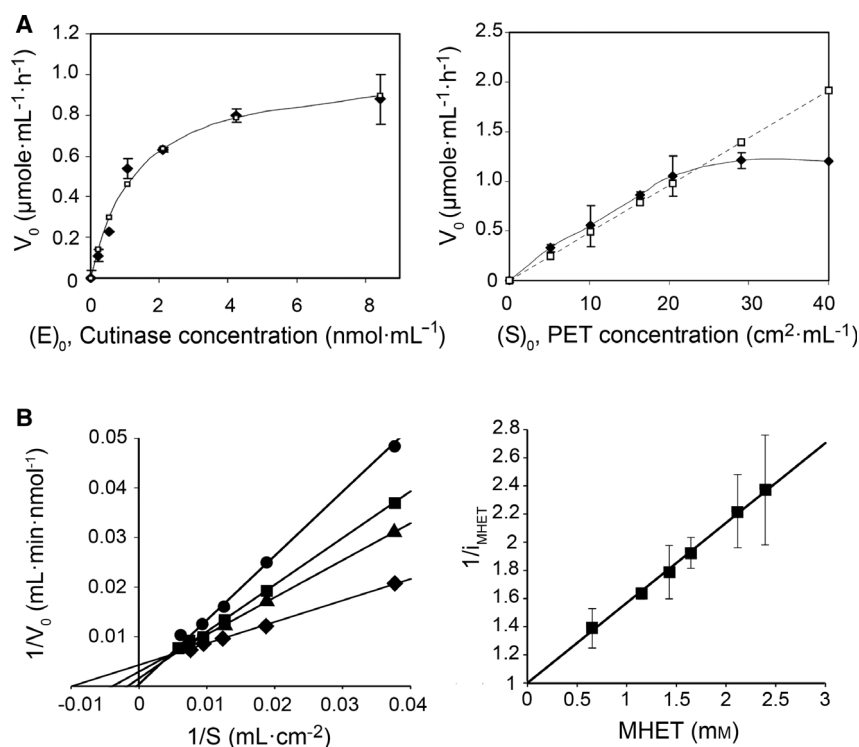
Fig. 3. Kinetics of a heterogeneous enzymatic reaction. Plot of the initial reaction rate of PET hydrolysis as a function of the concentration of the enzyme or the substrate. (A) Left: initial rate of PET hydrolysis as a function of *Pseudomonas mendocina* cutinase concentration at a fixed concentration of PET (13 cm^2·mL^{-1}). Data were fitted using eqn. 5. Right: initial rate of PET hydrolysis as a function of PET concentration at 2 μM *P. mendocina* cutinase. The rate of PET hydrolysis was measured by pH-stat and reported as added NaOH vs time at 50 °C. Experimental and fitted values were plotted as filled and open symbols, respectively. Figure in panel A is reproduced from Ref. [31]. (B) Inhibitory effect of the reaction of 50 μg·mL^{-1} TfCut2 by the product MHET. Left: double-reciprocal plots of the initial rates of PET hydrolysis as a function of the nanoparticle surface area in the presence of increasing concentrations of MHET. Right: plot of the inhibition parameter i_P as a function of the MHET concentration. The reactions were performed at a fixed nanoparticle surface of 80 cm^2·mL^{-1}, and data were fitted using the double reciprocal of eqn. 9. Figure in panel B is reproduced from Ref. [37].

A recent paper compared the hydrolytic rates of several cutinases and PETases by performing experiments under either enzyme saturation (at high substrate loads) or substrate saturation (at increasing enzyme concentration where all the accessible attack sites on the substrate surface are occupied) conditions, the latter yielding the so-called inverse Michaelis–Menten framework [29,33]. This approach allowed to calculate the density of attack sites, Γ_{attack}, on the PET surface in units of mol of sites per gram PET:

$$\frac{^{inv}V_{max}/S_0}{^{conv}V_{max}/E_0} = \Gamma_{attack} \qquad (7)$$

where $^{inv}V_{max}$ and $^{conv}V_{max}$ are the maximal rate from inverse and conventional M&M conditions, respectively, S_0 is the mass load of substrate (known), and E_0 is the amount of enzyme (known). Γ_{attack} was used to calculate $^{conv}K_m$ in molar units (i.e., $^{molar}K_m = {}^{conv}K_m\Gamma_{attack}$)

and thus the molar specificity constant (i.e., $^{molar}\eta = k_{cat}/^{molar}K_m$).

The very low $^{molar}K_m$ values for *Humicola insolens* and *Thermobifida fusca* cutinases on PET ($\sim$ 30 -40 nM) point to a very strong substrate interaction that could be mediated by a nonspecific adsorption to the PET surface. This conclusion is also supported by the observed high $^{molar}\eta$ values (in the 10^5–10^7 M^{-1}·s^{-1} range): the nonspecific adsorption on the hydrophobic surface of the substrate particles concentrates the enzyme near the attack sites and hence yields a higher effective substrate concentration than bulk reaction [33].

As for the canonical M&M kinetic model, the substrate-limited kinetic model can also be modified to account for a product inhibition effect. In this case, the inhibition parameter i_P, specific for each soluble inhibiting product (e.g., MHET), must be added to eqn. 5 (for details, see Ref. [36]):

$$v_0 = k_2 \frac{K_A A_0 [E]}{(1/i_p) + K_A A_0} \qquad (8)$$

The i_P parameter is related to the association constant for the formation of the enzyme–product complex (K_P) and to the [P] by the relationship:

$$i_p = \frac{1}{1 + K_P [P]} \qquad (9)$$

The proposed inhibition equation was used to investigate the inhibition of TfCut2 due to the accumulation of small soluble products (TPA, EG, MHET, and BHET) during the enzymatic hydrolysis of PET nanoparticles (nanoPET) (Fig. 3B) [36]. This study revealed that, although BHET and MHET showed similar K_p values (0.57 and 0.55 mm^{-1}, respectively), MHET had a higher inhibitory effect on the overall hydrolysis of nanoPET since it also originated from the other reaction product, that is, from BHET [36]. Since TPA and EG did not affect the enzyme hydrolysis of PET, the observed inhibition caused by MHET and BHET is probably due to their ester bonds that occupy the TfCut2 substrate binding site [36]. The same kinetic model was also applied to demonstrate that by using a dual-enzyme system, consisting of TfCut2 and an immobilized carboxylesterase from *T. fusca* KW3, MHET could be fully eliminated from the reaction mixture, thus relieving its inhibitory effect. The dual-enzyme system was 2.4-fold more efficient in hydrolyzing PET than the cutinase alone [37]. By using the same model, it was demonstrated that the improved PET hydrolytic efficiency of the G62A variant of TfCut2 was due to its lower affinity for the product MHET (5.5-fold lower i_P) than for the wild-type enzyme [38]. Comparison of the turnover number of cutinases and *I. sakaiensis* PETase for soluble fragments (MHET and BHET) vs intact PET indicates the interaction between the polymer strands in the solid PET as a slow (rate limiting) process, while the hydrolytic reaction itself could be fast [33]. The proposed kinetic model is based on the assumption that the enzyme acts at an internal ester bond of the polymer (i.e., it performs an endohydrolytic activity, and consequently, in turnover, a release-and-binding process is required to catalyze the following reaction cycle). On the other hand, it has been reported that during the hydrolysis of low crystalline PET, the enzyme could also show a processive-like exohydrolytic activity [24].

As stated by Ref. [33], 'The understanding of enzyme-catalyzed hydrolysis of PET and other plastics is not complete and there is no well-established framework for kinetic analyses of the reaction'.

Assays based on spectrophotometric methods

As proposed by Ref. [39], since hydrolysis of PET generates heterogeneous products, in terms of hydrophobicity and size, the use of a combination of several detection methods is strongly suggested. Variability in PET degradation assay results can arise from endolytic hydrolysis generating insoluble products as compared to exolytic activity or endolytic cleavages producing soluble monomers or small soluble fragments [24].

Spectrophotometric methods have been developed to assay the products arising from the enzymatic hydrolysis of PET. These methods are based on detecting changes in the absorbance of the reaction mixture due to production of compounds that absorb light (direct method) or on measuring the absorbance changes due to a suitable pH indicator dye (indirect method). In addition, changes in turbidity of the reaction mixture can also be used for this purpose (turbidimetric method). The activity detected by applying spectrophotometric methods might merely be a result of hydrolysis of molecules on the surface of PET particles (hydrophilization) and not from degradation of its core. For this reason, it is advisable to perform control experiments omitting the enzyme and combining the spectroscopic determination of PET hydrolysis with determinations of weight loss of the PET sample and/or with morphological analysis by scanning electron microscopy [40,41].

Direct methods

Colorimetric determination of hydrolysis of p-nitrophenol esters

The compounds pNPA and pNPB are classical substrates that can be used to detect different esterase activities, in particular lipases and hydrolases [42]. These enzymes catalyze the hydrolysis of ester bonds between an acyl moiety and *p*-nitrophenol (pNP): The release of 4-nitrophenolate anion (yellow at pH values above its pK$_a$ of 7.08 at 22 °C) is determined as a strong increase in absorbance at 405 nm (molar extinction coefficient = 18600 m^{-1}·cm^{-1}) [43]. Owing to the simple setup of this reaction, it can be used for the routine assay of enzymatic preparations (e.g., during the purification procedures) and for the determination of the ratio of active vs inactive clones as a result of a random mutagenesis procedure. In addition, the use of *p*-nitrophenol esterified with fatty acids of different chain length is helpful for probing the size of the enzyme active site and for determining the substrate

scope of hydrolases active on large linear substrates, such as cutinases. As an example, pNP monoesters of fatty acids with acyl chain lengths from 2 carbons (pNP-acetate) to 18 carbons (pNP-stearate) were used to determine the substrate scope of the recombinant LC-cutinase [43]. The substrates were evaluated in the presence of up to 10% acetonitrile to improve solubility. A specific activity of 270 U·mg^{-1} at pH 8.5 and 50 °C on pNP-butyrate for LC-cutinase was determined, which compared with a figure of 399 U·mg^{-1} for TfCut2 [43,44].

The major drawback of this assay is the low structural similarity between the PET polymer and pNP esters, which hampers identification of the PET hydrolytic enzymes. In addition, a significant autohydrolysis of the substrate at high temperatures and pH > 8.5 is observed [43]. The use of 15% poly(ethylene glycol) (PEG6000) during the pNP assay avoids adsorption of proteins to the plastic vials [32].

UV absorption detection of soluble compounds

The increase in absorbance of the reaction mixtures in the ultraviolet region of the light spectrum (at 240 nm) indicates the release of soluble TPA or its esters (BHET and MHET) from an insoluble PET substrate. These compounds share an identical strong absorbance peak around 240–244 nm with an identical extinction coefficient ($\varepsilon_{240 \text{ nm}} \sim 13800$ M^{-1}·cm^{-1}) as all three compounds contain the same number of carbonyl groups (Fig. 1) [40,45]. For this reason, the absorbance value at this wavelength can be used to calculate the overall sum of PET hydrolysis products according to the Lambert–Beer law (i.e., $[\text{Products}] = E_{240\text{nm}}/(\varepsilon_{240\text{nm}} \cdot l)$), and the enzyme-specific activity is determined as total equivalent of produced TPA [18,46]. Measurements can be performed by withdrawing aliquots of the reaction mixture at specific time intervals and transferring them into quartz cuvettes or UV-transparent plate wells (12–96 wells). To rule out interference due to the presence of other compounds that absorb the UV light, it is recommended that the absorbance spectrum of the reaction mixture be recorded from 220 to 300 nm instead of recording the absorbance intensity at a single wavelength.

This method has been applied to measure the release of PET hydrolysis products from a relatively large PET sample such as 10- to 15-mm circular (or square) swatches of PET film [40,45], 5-mm pieces of PET yarn, and 4- to 6-mm PET granulate [47]. As the reaction on these substrates is usually quite slow, measurements are performed from a minimum of few hours to several days: For analysis of the hydrolytic activity of

bacteria, the possibility that the products can be consumed by the microorganism themselves as a carbon source should be taken into consideration.

The main advantages of this method are that it can used both on whole microorganisms (e.g., actinomycetes) [47] and on purified enzymes [45] and that it does not require any sample processing (e.g., derivatization). The major limitations of this approach are that: (a) it can be applied on relatively large PET particles as substrate only (from microparticles up to larger PET fragments) because a fast and easy physical separation of the insoluble PET substrate from the soluble products is required before the spectrum can be spectrophotometrically recorded; (b) it is a discontinuous method; (c) in some cases, artifacts have been observed (e.g., an absorbance change in the first two hours due to absorption of the enzyme onto the fibers) [47,48]; and (d) it cannot be used when UV-absorbing compounds are present, for example, DMSO. In addition, a potential discrepancy between the measured and the actual reaction rates could arise from the heterogeneity of the reaction products; in particular, production of long insoluble oligomers or release of soluble dimers or short oligomers could result into the under- or overestimation of the reaction rate, respectively [39].

Indirect colorimetric assay based on the halochromic compound phenol red

The hydrolysis of PET produces small soluble compounds (BHET, MHET, and TPA) that possess free carboxylic groups (Fig. 1) and that, when accumulated, cause the pH of the reaction mixture to decrease (under low buffering conditions). The simplest method to measure the change in pH during the progress of the reaction is by using halochromic chemical compounds (i.e., acid–base indicators). The most common acid–base indicator is phenol red (phenolsulfonphthalein). This compound possesses an absorbance spectrum with two main peaks, at 550 and 430 nm (Fig. 4A). The pH decrease from 8.2 to 6.2 due to the accumulation of acidic reaction products changes the relative intensity of these peaks and causes a gradual transition from fuchsia to yellow [49]. This assay method can be used to monitor the reaction progress in a spectrophotometer cuvette or can even be adapted to perform a rapid and preliminary solid-phase screening of esterase screening microorganisms. As an example, it has been used for the identification of cutinase activities [50]. Clones were plated on agar medium containing the desired substrate (e.g., 1% cutin): The diffusion of the acidic reaction products lowered the

pH around the colony altering the color of the dye. The radius and intensity of the colored halo were proportional to the activity and the enzyme expression level. A trade-off between the optimal temperature of the hydrolysis reaction and the optimal growth temperature of the microorganism is required. Due to this limitation, the phenol red assay is more suited for the assay of the hydrolytic activity of purified enzymes on insoluble PET samples. In this case, the assay is performed in liquid phase (e.g., in an Eppendorf or a microtitration plate) and the supernatant can be easily separated from the insoluble substrate by a rapid centrifugation step. The reaction must be performed using a low-concentration buffer, since, at a high buffer concentration, the pH buffering power might decrease the assay sensitivity (for an example of experimental conditions, see legend of Fig. 4B). It is possible to estimate the specific activity of the tested enzyme sample by converting the $\Delta A_{550nm} \cdot min^{-1}$ in $U \cdot mg^{-1}$ enzyme using the extinction coefficient at 550 nm of phenol red ($8450 \ M^{-1} \cdot cm^{-1}$). Values must be corrected for the background nonenzymatic hydrolysis of the substrate.

Turbidimetric methods

Production of PET nanoparticles

Due to the compact nature of solid PET, PET hydrolases do not penetrate the polymer particles; consequently, the only PET ester bonds accessible to the enzyme are the ones on the surface of the polymeric particle. One strategy for increasing the reaction rate of the enzymatic hydrolysis is to use nanoPET whose

surface/mass ratio is very high (e.g. the surface/mass ratio for a PET nanoparticle of 100 nm in diameter is about 3000-fold higher than the corresponding value for a PET microparticle of 300 μm in diameter).

PET nanoparticles are not commercially available, but they can be produced according to a protocol that is quite straightforward [51,52]. The starting polymer (e.g., commercial PET microparticles or PET granulate, films, or fibers) is dissolved in the water-soluble solvent hexafluoro-2-propanol (100 mL of solvent for 1 g of PET). The polymer solution is then added drop by drop to a 10-fold larger volume of distilled water under vigorous stirring (e.g., using a homogenizer, at 8000 r.p.m., or a magnetic stirrer). The dilution of the polymer solution in water causes the formation of the nanoPET. Larger particles are removed by filtration, and the solvent is removed from the mixture using a rotatory evaporator as its boiling point (58.2 °C) is lower than that of water. The nanoparticle concentration is determined by weighing the PET contained in an aliquot of nanoparticle solution (from 1 to 10 mL) after harvesting by centrifugation and drying at 40 °C for 24 h (Fig. 5A). The resulting concentration in the suspension should usually be $< 6 \ mg \cdot mL^{-1}$ since flocculation or film formation occurs at a higher concentration. The particle size, determined by dynamic light scattering, is usually in the 50- to 250-nm range [51].

An alternative protocol for the preparation of nanoPET was recently proposed [52]. According to this protocol, 1 g of fine debris of PET (< 0.2 mm, obtained from soft drink bottles) was dissolved in 10 mL of 90% v/v trifluoroacetic acid solution (TFA) at 50 °C. The solution was stirred until the PET debris
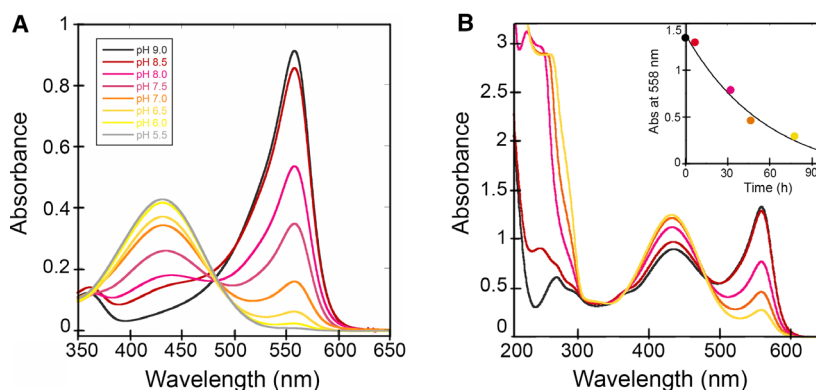

Fig. 4. Colorimetric assay of PET hydrolysis using the halochromic compound phenol red. (A) Changes in the absorbance spectrum of phenol red as a function of pH. (B) Absorbance spectra of the supernatant of the enzymatic hydrolysis reaction of PET microparticles (diameter: 300 μm). The increase at 240 nm is due to the accumulation of soluble products in the reaction supernatant. Inset: variation of absorbance at 558 nm during the reaction time course (data were interpolated using a single exponential decay equation). Reaction conditions: 8.5 $mg \cdot mL^{-1}$ PET microparticles, 18.5 $\mu g \cdot mL^{-1}$ *Ideonella sakaiensis* PETase, 0.075 mM phenol red, 37 °C. Buffer: 1 mM Na_2HPO_4 and 100 mM NaCl, pH 8.1.
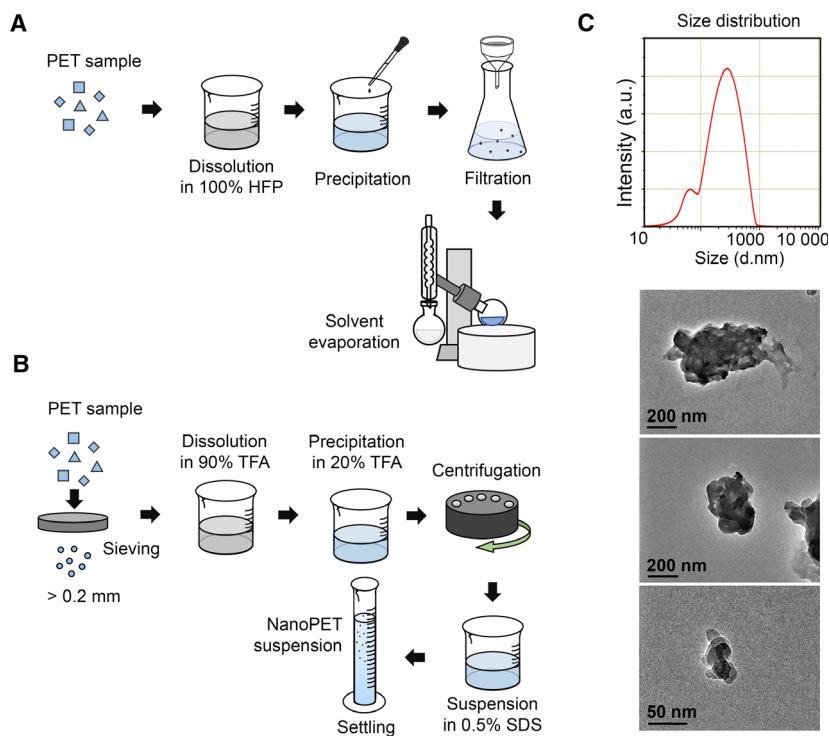
Fig. 5. Overview of the protocols for preparing nanoPET. (A) Production of nanoparticles by diluting PET, solubilized with hexafluoro-2-propanol, with distilled water under vigorous stirring. (B) Production of nanoparticles by solubilizing PET into TFA followed by dilution into aqueous solution of TFA (20% v/v) under stirring, and then separating by sedimentation. (C) Dynamic light-scattering analysis of nanoPET in aqueous solution (top) and clusters of nanoPET photographed by transmission electron microscopy (bottom). Figure in panel C is reproduced from Ref. [52].

had completely dissolved (~ 2 h). Nanoparticles were formed by adding 10 mL of a diluted aqueous solution of TFA (20% v/v) to the initial mixture (that had settled overnight) under stirring for 2 h. Nanoparticles were collected by centrifugation, resuspended in 100 mL of 0.5% sodium dodecyl sulfate, and subjected to stirring and ultrasonication to obtain a homogeneous suspension. PET particles larger than 300 nm were separated by sedimentation in a cylinder (for 1 h) and nanoPET ranging from 50 to 300 nm (as determined by dynamic light scattering) were recovered in the upper portion of the solution (Fig. 5B,C). The nanoPET showed the same chemical structure as the original material (analyzed by Fourier transform infrared spectroscopy) and could be kept in suspension for several days or stored as dry powder [52].

Turbidimetric analysis of hydrolysis of PET nanoparticles (nanoPET)

Dispersion of nanoPET in an aqueous solvent generates a heterogeneous colloid mixture that scatters visible light due to the Tyndall effect (Fig. 6A). The resulting turbidity of the solution, which can be easily measured by recording the optical density of the solution at 600 nm (OD_{600}) using a spectrophotometer, is related to the concentration of the particles (Fig. 6B) [53]. During enzymatic erosion of nanoPET particles,

the OD_{600} of the solution decreases owing to the decrease in size and number of nanoparticles in suspension at a rate directly proportional to the enzymatic activity [32]. As an example, 0.3 mg·mL^{-1} of nanoPET produced using PET from different sources (from granulate, film, or fibers) was treated with increasing concentrations of TfCut2 (up to 50 μg·mL^{-1}): The turbidity of the reaction mixture reached a value < 5% after 30 min of incubation at 60 °C with the exception of the one produced from recycled PET granulate. This nanoparticle preparation corresponds to a PET concentration of 8.6 μM and a concentration of ester bonds of 1.57 mM (considering an estimated mean degree of polymerization of amorphous PET of 181.7 units and a MW of 35 000 g·mol^{-1}) [25]; anyway, only the ester bonds exposed on the nanoparticle surface are available for the enzymatic hydrolysis. To avoid sedimentation of nanoparticles with a diameter > 100 nm during the reaction and to increase the reproducibility of the measurements, nanoPET were immobilized onto 0.9% agarose matrix with pore sizes between 100 and 250 nm [32]. Recently, the same group applied the turbidimetric method to measure the activity of PET-hydrolyzing enzymes on other substrates, that is, BHET and ethylene glycol bis-(*p*-methylbenzoate) (2PET). These substrates were used in a nanoparticle form in assays performed on microplates, demonstrating the
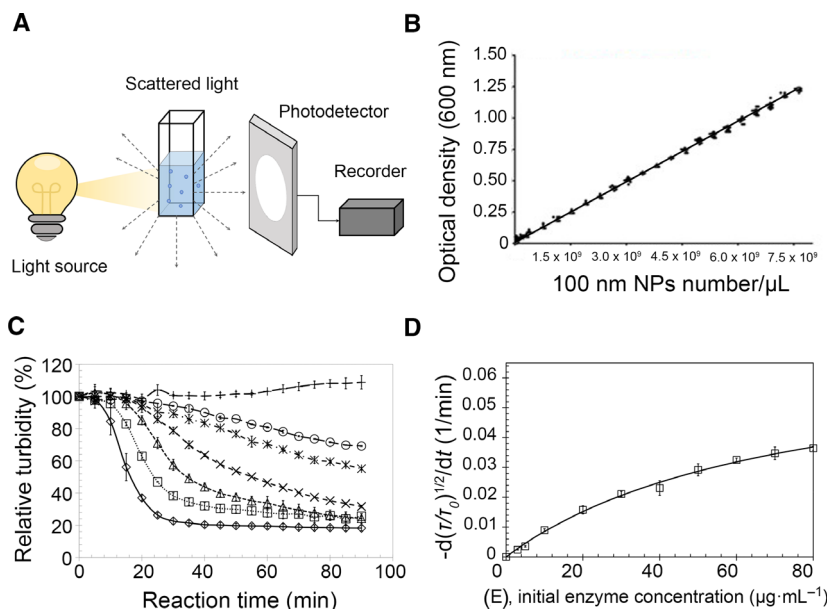
Fig. 6. Turbidimetric analysis of the enzymatic hydrolysis of nanoPET. (A) NanoPET (with a diameter of ~ 50–300 nm) suspended in an aqueous solution scatter the light due to the Tyndall effect. The intensity of the scattered light is inversely proportional to the fourth power of the wavelength. (B) The OD_{600} value of a solution of nanoPET is linearly dependent on the number of nanoparticles suspended and on their diameter. Figure reproduced from Ref. [53]. (C) Time course of the turbidity (OD_{600}) decrease of a preparation of agarose-immobilized nanoPET from recycled PET granulate (0.2 mg·mL^{-1}) incubated with TfCut2 (the enzyme concentration was in the 3- to 50-µg·mL^{-1} range). Figure reproduced from Ref. [32]. (D) The initial reaction rates reported as the square roots of turbidity decrease, calculated from the linear region of the curves reported in panel C, as a function of the concentration of TfCut2. Experimental data were fitted using eqn. 10 (solid curve). Figures in panels B–D are reproduced from Ref. [32].

possibility of applying this method to rapid screening protocols, too. In this assay, the nanoparticles were entrapped in a matrix of 4.5% acrylamide (with pore size of ~ 0.2 µm) containing the enzyme. The turbidity decrease was followed at 60 °C up to 10 or 120 min for BHET or 2PET, respectively [54]. A similar approach was also used to monitor the progress of the enzymatic degradation of a suspension of nanoparticles of the biodegradable polymer poly(butylene succinate-co-adipate) [40,41].

Analysis of turbidimetric data

Experimental data obtained from turbidimetric measurements and expressed as v_0 as a function of the initial enzyme concentration ([E]) can be interpolated using an alternative form of eqn. 5, where v_0 is expressed as the rate of change in turbidity (for details, see Ref. [32]):

$$v_0 = -\frac{d(\sqrt{\tau})}{dt} = k_\tau \frac{K_A[E]}{1 + K_A[E]} \qquad (10)$$

According to eqn. 10, the relative hydrolysis rate constant (k_τ) and the enzyme adsorption equilibrium constant (K_A) can be determined from interpolation of the initial reaction rate values $-\frac{d(\sqrt{\tau})}{dt}$ as a function of [E]. The absolute hydrolysis rate constant is obtained as a ratio of k_τ and the initial overall surface area of the nanoparticles ($k = k_\tau / A_0$). The k, k_τ, and K_A are relevant parameters for defining the performances of a specific enzyme on different nanoPET (e.g., nanoparticles produced from different polymers or of different sizes).

This model was applied to investigate the hydrolysis of nanoparticles formed by aggregated BHET or 2PET molecules catalyzed by the carboxylesterase TfCa from *Thermobifida fusca* KW3. Analysis of the kinetic data showed that the esterase activity (represented by the k_τ parameter) correlated with the accessibility of the enzyme active site. The k_τ for the smallest substrate (BHET) was ~ 3.5-fold higher than that for the largest compound (2PET) [54]. The same kinetic parameter was taken into account to demonstrate that the two paralogous polyester hydrolases expressed in *Thermomonospora curvata* possess a > 10-fold higher activity on poly(ε-caprolactone) than on PET [32].

The K_A parameter is also useful to evaluate the activity of an esterase on different polymers. For example, the polyester hydrolase TfCut2 shows similar

k_τ values but different K_A values for the hydrolysis of alternative nanoPET (i.e., nanoparticles produced from recycled PET granulate, film, or fibers): Researchers proposed that the efficiency of the enzymatic degradation was mostly controlled by the adsorption equilibrium constant (i.e., by the affinity of the enzyme for the superficial ester bonds of the substrate) [32].

Fluorimetric methods

Enzymatic assays based on detecting fluorescent products are generally more sensitive than the spectrophotometric ones, require a more stringent control of the assay temperature, and are more prone to chemical interference. A preliminary investigation concerning the quantitation of the TPA produced by the enzymatic hydrolysis of PET showed that this compound can be quantitatively converted to hydroxyphthalic acid (HOTH or HTA) by the reaction with hydrogen peroxide under boiling conditions [55]. HOTH can be detected by measuring fluorescence at 421 nm (excitation at 328 nm) [56].

A more recent and reliable protocol based on the fluorimetric detection of the same compound generated by free hydroxyl radicals produced by iron autoxidation at room temperature (a modified Fenton reaction) is described in Fig. 7 [57,58]. Molecular oxygen dissolved in the assay mixture (~ 0.24 mM at room temperature) reacts with Fe(II) to produce the superoxide (O_2^-) ion. Two superoxide ions react to form one molecule of hydrogen peroxide that, in turn, is further reduced by Fe(II) with the production of one hydroxyl radical ($^\bullet OH$). This latter species readily reacts with TPA, producing HOTH. An incubation time of ~ 6 min is required to allow full TPA hydroxylation; the fluorescence signal is stable for > 24 h [59]. This assay protocol can be performed both in cuvettes (3 mL assay final volume) or in microplate wells (150 μL assay final volume); its fluorescence signal is linear from 0.01 to 0.075 mM TPA (in 0.1 M phosphate buffer, pH 8.5) [58]. Neither proteins nor microorganisms interfere in fluorescence emission in the sample assays; thus, this method can be used to assay PET

hydrolytic reactions without requiring any preliminary treatment of the sample [60]. A further major advantage of this method, in comparison with the spectrophotometric detection of the PET hydrolysis products at ~ 240 nm, is its specificity for detecting TPA as both MHET and BHET do not react with the hydroxyl radical [58].

This approach was recently exploited for screening a microbial library for enzymes active on PET on microplates (final volume of 200 μL). By adding exogenous H_2O_2 to the assay mixture (130 mM), the limiting starting O_2 concentration (0.24 mM) could be overcome: Owing to the increase in H_2O_2 concentration, the linear detection range of TPA could be extended up to 0.5 mM [60].

Titrimetric methods

In a titrimetric method, the optimal pH value for a specific reaction that produces dissociable compounds is maintained constant by a device (pH-Stat) that adds the required amount of an acid or alkaline reagent. The kinetics of the reaction of interest is then calculated based on the consumption (as a function of time) of the neutralizing reagent. This method is particularly suitable for investigating the catalytic hydrolysis of PET, which produces compounds possessing one or two carboxylic groups such as TPA, MHET, and BHET (Fig. 1) [34]. The titrimetric method was applied to assay the enzymatic activity of different cutinases on PET samples (such as 5 × 5-mm PET films). The reaction was followed for ~ 1 h, and the slopes (expressed as micromoles of added NaOH/mL of reaction volume/hour) were measured in the linear region of the curve (from 15 to 30 min), making it possible to assess cutinase activity under different conditions (e.g., different temperature or pH). The rates of PET hydrolysis were plotted as a function of the enzyme or PET concentration and were interpolated using eqn. 5 [31].

Recently, a titrimetric assay was used to investigate the catalytic performances of several multiple variants of the leaf-branch compost cutinase (LCC) [46]. The
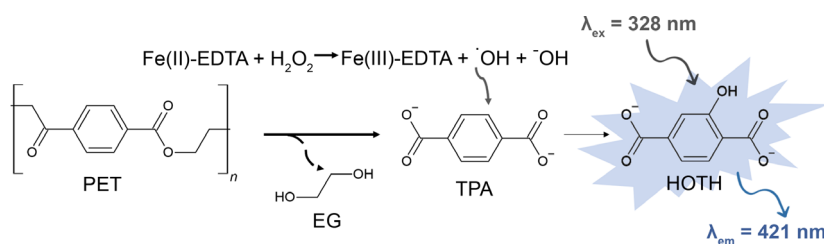

Fig. 7. Fluorimetric assay of the PET enzymatic hydrolysis.

reactions were performed in a 500-mL bioreactor equipped with a thermostat: pH was maintained constant at 8 by adding 6 N NaOH. The reaction mixture, constituted by 20 g of postconsumer colored-flake PET waste (PcW-PET), was added to 80 mL reaction volume containing up to 2.07 μmol of purified enzyme. Both the depolymerization yield and the initial rate of the reaction ($g_{(hydrolyzed\ PET)}$ L^{-1}·h^{-1}) were calculated according to the amount of NaOH consumption [46]. The authors demonstrated that the F243I/D238C/S283C/Y127G and F243W/D238C/S283C/Y127G variants of LCC were able to hydrolyze 82% and 85% of PET granulate, respectively, while wild-type LCC only reached 53% conversion. The optimal incubation temperature and enzyme concentration were identified to maximize the cost–productivity ratio in a potential industrial recycling application [46].

HPLC

Reverse-phase HPLC systems have been widely used to analyze the products derived from the enzymatic hydrolysis of PET owing to its powerful resolving capability and reproducibility. The different compounds produced by PET hydrolytic enzymes (i.e., TPA, MHET, and BHET) can be efficiently separated on a C18 reverse-phase HPLC column: The reaction mixture is loaded into a column equilibrated with a polar mobile phase, and the concentration of the organic solvent (acetonitrile) [18,27,43,61–63] or methanol [11,46,64,65] is increased over time (gradient elution). The pH of the mobile phase is kept constant during the run. Elution of TPA and its esters is followed by measuring the UV absorbance of the eluate in the 240- to 244-nm range due to the presence of the two carbonyl groups [31]. Elution of products can also be recorded in the 254- to 260-nm range due to the absorbance of the TPA aromatic ring [27,63]. The reaction product showing the lowest retention time is TPA, while the one with the highest retention time is BHET (Fig. 8).

Although HPLC is a discontinuous assay and is more time-consuming than other procedures, it is the only method that gives the exact amount of each reaction product, provided that suitable standards are available. While TPA and BHET are commercially available, MHET needs to be synthetized; a protocol for the synthesis of MHET is reported by Ref. [46]. This approach is prone to the same potential issue of under- or overestimation of the reaction rate due to the heterogeneous solubility of the reaction products commented above (see UV absorption detection of soluble compounds paragraph) [39].
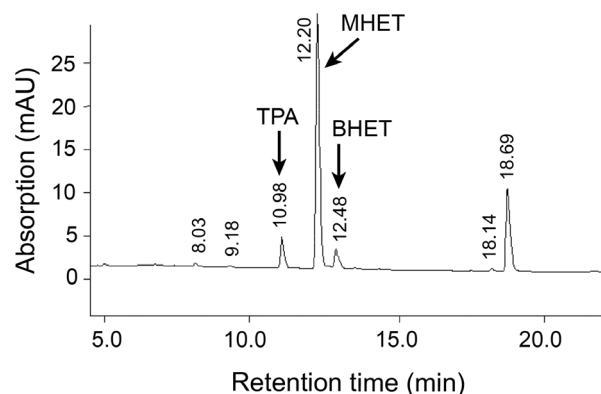

Fig. 8. Reverse-phase HPLC separation of reaction products of the enzymatic hydrolysis of PET. PET granules (5.0 g) were treated with cutinase from *Fusarium solani pisi* (25 U) in 25 mM phosphate buffer (pH 8) at 30 °C for 24 h, and reaction products were separated on a Chrompack C18 column. The polar mobile phase (1% TFA solution in water) was gradually substituted with acetonitrile, applying a linear gradient from 1% TFA solution at the start of the run to 10% of 1% TFA and 90% of acetonitrile at the end of the run (separation length: 30 min). Figure reproduced from Ref. [18].

Discussion

The discovery of novel microorganisms that use PET as a major carbon and energy source has raised interest both for their application in bioremediation and for elucidation of the mechanism(s) of the related enzymes. Furthermore, the natural enzymes active on PET represent valuable scaffolds for additional protein engineering studies aimed at increasing the efficiency and substrate acceptance for degrading such a highly resistant polymer. Both these approaches require simple and accurate analytical methods that, moving from artificial/simple model compounds, can evaluate the enzymatic potential on PET samples. To reach the industrial level, the enzymatic treatment of PET materials requires highly active and stable enzymes (to shorten the treatment times) and enzymes that are not sensitive to product inhibition effects. Here, the use of multienzymatic systems seems a useful approach to perform the continuous hydrolysis of PET [37], a process that once again requires an in-depth evaluation of the kinetics.

Acknowledgements

student of the 'Life Sciences and Biotechnology' course at Università degli Studi dell'Insubria.

Conflict of interest

The authors declare no conflict of interest.

Author contributions

All authors helped in writing the manuscript and have given approval to the final version of the manuscript.

References

1 Law KL (2010) Plastic accumulation in the north. *Science* **80**, 1185–1188.

2 Cózar A, Echevarría F, González-Gordillo JI, Irigoien X, Úbeda B, Hernández-León S, Palma ÁT, Navarro S, García-de-Lomas J, Ruiz A *et al.* (2014) Plastic debris in the open ocean. *Proc Natl Acad Sci USA* **111**, 10239–10244.

3 Jambeck J, Geyer R, Wilcox C, Siegler TR, Perryman M, Andrady A, Narayan R & Law KL (2015) Plastic waste inputs from land into the ocean. *Mar Pollut* **347**, 768–771.

4 Geyer R, Jambeck JR & Law KL (2017) Production, use, and fate of all plastics ever made. *Sci Adv* **3**, 25–29.

5 Worm B, Lotze HK, Jubinville I, Wilcox C & Jambeck J (2017) Plastic as a persistent marine pollutant. *Annu Rev Environ Resour* **42**, 1–26.

6 Gallagher FG (2003) Controlled degradation polyesters. In Modern Polyesters: Chemistry and Technology of Polyesters and Copolyesters (Scheirs J & Long TE, eds), pp. 591–608. John Wiley & Sons, Chichester, UK.

7 Paszun D & Spychaj T (1997) Chemical recycling of poly(ethylene terephthalate). *Ind Eng Chem Res* **36**, 1373–1383.

8 Fukushima K, Coulembier O, Lecuyer JM, Almegren HA, Alabdulrahman AM, Alsewailem FD, McNeil MA, Dubois P, Waymouth RM, Horn HW *et al.* (2011) Organocatalytic depolymerization of poly (ethylene terephthalate). *J Polym Sci A* **49**, 1273–1281.

9 Spaseska D & Civkaroska M (2010) Alkaline hydrolysis of poly(ethylene terephthalate) recycled from the postconsumer soft-drink bottles. *J Univ Chem Technol Metall* **45**, 379–384.

10 Restrepo-Flórez JM, Bassi A & Thompson MR (2014) Microbial degradation and deterioration of polyethylene - A review. *Int Biodeterior Biodegrad* **88**, 83–90.

11 Yoshida S, Hiraga K, Takanaha T, Taniguchi I, Yamaji H, Maeda Y, Toyohara K, Miyamoto K, Kimura Y & Oda K (2016) A bacterium that degrades and assimilates poly(ethylene terephthalate). *Science* **80**, 1196–1199.

12 Bombelli P, Howe CJ & Bertocchini F (2017) Polyethylene bio-degradation by caterpillars of the wax moth *Galleria mellonella*. *Curr Biol* **27**, R292–R293.

13 Dvořák P, Nikel PI, Damborský J & de Lorenzo V (2017) Bioremediation 3.0: engineering pollutant-removing bacteria in the times of systemic biology. *Biotechnol Adv* **35**, 845–866.

14 Nimchua T, Punnapayak H & Zimmermann W (2007) Comparison of the hydrolysis of polyethylene terephthalate fibers by a hydrolase from *Fusarium oxysporum* LCH I and *Fusarium solani* f. sp. *pisi*. *Biotechnol J* **2**, 361–364.

15 Nimchua T, Eveleigh DE, Sangwatanaroj U & Punnapayak H (2008) Screening of tropical fungi producing polyethylene terephthalate- hydrolyzing enzyme for fabric modification. *J Ind Microbiol Biotechnol* **35**, 843–850.

16 Zheng Y, Yanful EK & Bassi AS (2005) A review of plastic waste biodegradation. *Crit Rev Biotechnol* **25**, 243–250.

17 Müller RJ, Schrader H, Profe J, Dresler K & Deckwer WD (2005) Enzymatic degradation of poly(ethylene terephthalate): rapid hydrolyse using a hydrolase from *T. fusca*. *Macromol Rapid Commun* **26**, 1400–1405.

18 Vertommen MAME, Nierstrasz VA, Van Der VM & Warmoeskerken MMCG (2005) Enzymatic surface modification of poly(ethylene terephthalate). *J Biotechnol* **120**, 376–386.

19 Araújo R, Silva C, O'Neill A, Micaelo N, Guebitz G, Soares CM, Casal M & Cavaco-Paulo A (2007) Tailoring cutinase activity towards polyethylene terephthalate and polyamide 6,6 fibers. *J Biotechnol* **128**, 849–857.

20 Herrero Acero E, Ribitsch D, Steinkellner G, Gruber K, Greimel K, Eiteljoerg I, Trotscha E, Wei R, Zimmermann W, Zinn M *et al.* (2011) Enzymatic surface hydrolysis of PET: Effect of structural diversity on kinetic properties of cutinases from *Thermobifida*. *Macromolecules* **44**, 4632–4640.

21 Ribitsch D, Acero EH, Greimel K, Eiteljoerg I, Trotscha E, Freddi G, Schwab H & Guebitz GM (2012) Characterization of a new cutinase from *Thermobifida alba* for PET-surface hydrolysis. *Biocatal Biotransformation* **30**, 2–9.

22 Sharon C & Sharon M (2012) Studies on biodegradation of polyethylene terephthalate: a synthetic polymer. *J Microbiol Biotechnol Res* **2**, 248–257.

23 Zimmermann W & Billig S (2011) Enzymes for the biofunctionalization of poly(ethylene terephthalate). *Adv Biochem Eng Biotechnol* **125**, 97–120.In *Biofunctionalization of Polymers and their Applications*. Springer, Berlin, Heidelberg.

24 Wei R, Breite D, Song C, Gräsing D, Ploss T, Hille P, Schwerdtfeger R, Matysik J, Schulze A & Zimmermann

W (2019) Biocatalytic degradation efficiency of postconsumer polyethylene terephthalate packaging determined by their polymer microstructures. *Adv Sci* **6**, 1900491.

25 Falkenstein P, Gräsing D, Bielytskyi P, Zimmermann W, Matysik J, Wie R & Song C (2020) UV pretreatment impairs the enzymatic degradation of polyethylene terephthalate. *Front Microbiol* **11**, 689.

26 Falkenstein P, Wei R, Matysik J & Song C (2020) Mechanistic investigation of enzymatic degradation of polyethylene terephthalate by nuclear magnetic resonance. *Methods Enzymol* **648**, 231–252.

27 Joo S, Cho IJ, Seo H, Son HF, Sagong HY, Shin TJ, Choi SY, Lee SY & Kim KJ (2018) Structural insight into molecular mechanism of poly(ethylene terephthalate) degradation. *Nat Commun* **9**, 382.

28 Taniguchi I, Yoshida S, Hiraga K, Miyamoto K, Kimura Y & Oda K (2019) Biodegradation of PET: current status and application aspects. *ACS Catal* **9**, 4089–4105.

29 Kari J, Andersen M, Borch K & Westh P (2017) An inverse Michaelis-Menten approach for interfacial enzyme kinetics. *Acs Catal* **7**, 4904–4914.

30 Scandola M, Focarete ML & Frisoni G (1998) Simple kinetic model for the heterogeneous enzymatic hydrolysis of natural poly(3-hydroxybutyrate). *Macromolecules* **31**, 3846–3851.

31 Ronkvist ÅM, Xie W, Lu W & Gross RA (2009) Cutinase-catalyzed hydrolysis of poly(ethylene terephthalate). *Macromolecules* **42**, 5128–5138.

32 Wei R, Oeser T, Barth M, Weigl N, Lübs A, Schulz-Siegmund M, Hacker MC & Zimmermann W (2014) Turbidimetric analysis of the enzymatic hydrolysis of polyethylene terephthalate nanoparticles. *J Mol Catal B Enzym* **103**, 72–78.

33 Bååth JA, Borch K, Jensen K, Brask J & Westh P (2021) Comparative biochemistry of four polyester (PET) hydrolases. *ChemBioChem* **22**, 1–12.

34 Herzog K, Müller RJ & Deckwer WD (2006) Mechanism and kinetics of the enzymatic hydrolysis of polyester nanoparticles by lipases. *Polym Degrad Stab* **91**, 2486–2498.

35 Silva C, Da S, Silva N, Matamá T, Araújo R, Martins M, Chen S, Chen J, Wu J, Casal M *et al.* (2011) Engineered *Thermobifida fusca* cutinase with increased activity on polyester substrates. *Biotechnol J* **6**, 1230–1239.

36 Barth M, Oeser T, Wei R, Then J, Schmidt J & Zimmermann W (2015) Effect of hydrolysis products on the enzymatic degradation of polyethylene terephthalate nanoparticles by a polyester hydrolase from *Thermobifida fusca*. *Biochem Eng J* **93**, 222–228.

37 Barth M, Honak A, Oeser T, Wei R, Belisário-Ferrari MR, Then J, Schmidt J & Zimmermann W (2016) A dual enzyme system composed of a polyester hydrolase

and a carboxylesterase enhances the biocatalytic degradation of polyethylene terephthalate films. *Biotechnol J* **11**, 1082–1087.

38 Wei R, Oeser T, Schmidt J, Meier R, Barth M, Then J & Zimmermann W (2016) Engineered bacterial polyester hydrolases efficiently degrade polyethylene terephthalate due to relieved product inhibition. *Biotechnol Bioeng* **113**, 1658–1665.

39 Bååth JA, Borch K & Westh P (2020) A suspension-based assay and comparative detection methods for characterization of polyethylene terephthalate hydrolases. *Anal Biochem* **607**, 113873.

40 Kawai F, Oda M, Tamashiro T, Waku T, Tanaka N, Yamamoto M, Mizushima H, Miyakawa T & Tanokura M (2014) A novel Ca²⁺-activated, thermostabilized polyesterase capable of hydrolyzing polyethylene terephthalate from *Saccharomonospora viridis* AHK190. *Appl Microbiol Biotechnol* **98**, 10053–10064.

41 Oda M, Yamagami Y, Inaba S, Oida T, Yamamoto M, Kitajima S & Kawai F (2018) Enzymatic hydrolysis of PET: functional roles of three Ca²⁺ ions bound to a cutinase-like enzyme, Cut190*, and its engineering for improved activity. *Appl Microbiol Biotechnol* **102**, 10067–10077.

42 Syedd R, Sandoval M, Trimiño H, Villegas L & Rodríguez G (2020) Revisiting the fundamentals of p-nitrophenol analysis for its application in the quantification of lipases activity. A graphical update. *Uniciencia* **34**, 31–43.

43 Sulaiman S, Yamato S, Kanaya E, Kim JJ, Koga Y, Takano K & Kanaya S (2012) Isolation of a novel cutinase homolog with polyethylene terephthalate-degrading activity from leaf-branch compost by using a metagenomic approach. *Appl Environ Microbiol* **78**, 1556–1562.

44 Chen S, Tong X, Woodard RW, Du G, Wu J & Chen J (2008) Identification and characterization of bacterial cutinase. *J Biol Chem* **283**, 25854–25862.

45 Kellis JT Jr, Poulose AJ & Yoon MY (2001) Enzymatic modification of the surface of a polyester fiber or article. US Pat No 6,254,645 Washington, DC US Pat Trademark Off.

46 Tournier V, Topham CM, Gilles A, David B, Folgoas C, Moya-Leclair E, Kamionka E, Desrousseaux ML, Texier H, Gavalda S *et al.* (2020) An engineered PET depolymerase to break down and recycle plastic bottles. *Nature* **580**, 216–219.

47 Alisch M, Feuerhack A, Müller H, Mensak B, Andreaus J & Zimmermann W (2004) Biocatalytic modification of polyethylene terephthalate fibres by esterases from actinomycete isolates. *Biocatal Biotransformation* **22**, 347–351.

48 Gouda MK, Kleeberg I, Van den Heuvel J, Müller RJ & Deckwer WD (2002) Production of a polyester

degrading extracellular hydrolase from *Thermomonospora fusca. Biotechnol Prog* **18**, 927–934.

49 Reyes-Duarte D, Coscolín C, Martínez-Martínez M, Ferrer M & García-Arellano H (2018) Functional-based screening methods for detecting esterase and lipase activity against multiple substrates. *Methods Mol Biol* **1835**, 109–117.

50 Halonen P, Reinikainen T, Nyyssölä A & Buchert J (2009) A high throughput profiling method for cutinolytic esterases. *Enzyme Microb Technol* **44**, 394–399.

51 Welzel K (2003) Einfluss der chemischen struktur auf die enzymatische hydrolyse von polyester-nanopartikeln. *PhD dissertation*, 1–181.

52 Rodríguez-Hernández AG, Muñoz-Tabares JA, Aguilar-Guzmán JC & Vazquez-Duhalt R (2019) A novel and simple method for polyethylene terephthalate (PET) nanoparticle production. *Environ Sci Nano* **6**, 2031–2036.

53 Unciti-Broceta JD, Cano-Cortés V, Altea-Manzano P, Pernagallo S, Díaz-Mochón JJ & Sánchez-Martín RM (2015) Number of nanoparticles per cell through a spectrophotometric method - A key parameter to assess nanoparticle-based cellular assays. *Sci Rep* **5**, 1–10.

54 Belisário-Ferrari MR, Wei R, Schneider T, Honak A & Zimmermann W (2019) Fast turbidimetric assay for analyzing the enzymatic hydrolysis of polyethylene terephthalate model substrates. *Biotechnol J* **14**, 10–14.

55 O'Neill A & Cavaco-Paulo A (2004) Monitoring biotransformations in polyesters. *Biocatal Biotransformation* **22**, 353–356.

56 Fang X, Mark G & Von Sonntag C (1996) OH radical formation by ultrasound in aqueous solutions: Part I: the chemistry underlying the terephthalate dosimeter. *Ultrason Sonochem* **3**, 57–63.

57 Yang XF & Guo XQ (2001) Fe(II)-EDTA chelate-induced aromatic hydroxylation of terephthalate as a new method for the evaluation of hydroxyl radical-scavenging ability. *Analyst* **126**, 928–932.

58 Wei R, Oeser T, Billig S & Zimmermann W (2012) A high-throughput assay for enzymatic polyester hydrolysis activity by fluorimetric detection. *Biotechnol J* **7**, 1517–1521.

59 Saran M & Summer KH (1999) Assaying for hydroxyl radicals: hydroxylated terephthalate is a superior fluorescence marker than hydroxylated benzoate. *Free Radic Res* **31**, 429–436.

60 Chaves MRB, Lima MLSO, Malafatti-Picca L, De Angelis DA, De Castro AM, Valoni É & Marsaioli AJ (2018) A practical fluorescence-based screening protocol for polyethylene terephthalate degrading microorganisms. *J Braz Chem Soc* **29**, 1278–1285.

61 Liu B, He L, Wang L, Li T, Li C, Liu H, Luo Y & Bao R (2018) Protein crystallography and site-direct mutagenesis analysis of the poly(ethylene terephthalate) hydrolase petase from *Ideonella sakaiensis*. *ChemBioChem* **19**, 1471–1475.

62 Shirke AN, White C, Englaender JA, Zwarycz A, Butterfoss GL, Linhardt RJ & Gross RA (2018) Stabilizing leaf and branch compost cutinase (LCC) with glycosylation: mechanism and effect on PET hydrolysis. *Biochemistry* **57**, 1190–1200.

63 Carniel A, Valoni É, Nicomedes J, Gomes AC & Castro AM (2017) Lipase from *Candida antarctica* (CALB) and cutinase from *Humicola insolens* act synergistically for PET hydrolysis to terephthalic acid. *Process Biochem* **59**, 84–90.

64 Han X, Liu W, Huang JW, Ma J, Zheng Y, Ko TP, Xu L, Cheng YS, Chen CC & Guo RT (2017) Structural insight into catalytic mechanism of PET hydrolase. *Nat Commun* **8**, 2106.

65 Austin HP, Allen MD, Donohoe BS, Rorrer NA, Kearns FL, Silveira RL, Pollard BC, Dominick G, Duman R, El Omari K *et al.* (2018) Characterization and engineering of a plastic-degrading aromatic polyesterase. *Proc Natl Acad Sci USA* **115**, E4350–E4357.